

30  
7/16/87 JEM  
①

⑤

DR-0267-4

SLAC - PUB - 4182  
January 1987  
(A)

# TRANSVERSE WAKEFIELD CONTROL AND FEEDBACK IN THE SLC LINAC\*

J. T. SEEMAN, I. E. CAMPISI, W. HERRMANNFELDT, M. LEE, A. PETERSEN,  
N. PHINNEY, M. ROSS, R. STIENING, K. THOMPSON AND D. TSANG

Stanford Linear Accelerator Center, Stanford, California 94305

G. S. ABRAMS

Lawrence Berkeley Laboratory, Berkeley, California 94720

SLAC-PUB--4182

C. ADOLPHSEN

University of California, Santa Cruz, California 95064

DE87 011588

and

E. SODERSTROM

California Institute of Technology, Pasadena, California 91125

## Abstract

Transverse wakefields in the linac of the SLAC Linear Collider (SLC) have been observed to enlarge the effective emittance of beams which are not properly centered in the accelerating structure.<sup>1,2</sup> A fast feedback system has been constructed to minimize the enlargement under changing conditions by controlling the beam launching parameters. Theoretical aspects of this transverse feedback system are reviewed as well as the design of the beam sensors, launch controllers, communication equipment and data processing micro-computer. A variety of beam observations have been made. They show that dispersion as well as wakefield effects are important. In the near future the fast transverse feedback system will be beam tested, and algorithms tailored to the noise environment of the SLC will be tried.

## System Overview

The transverse feedback system of the linac has components for both slow and fast beam control. Trajectory correction over the entire linac<sup>2,3</sup> involving 550 dipoles and 275 beam position monitors (BPM) is performed about every 30 minutes. In this way, trajectory errors are kept below 200  $\mu\text{m}$  rms. Linac input and output launch parameters ( $x, x', y, y'$ ) are corrected<sup>3</sup> about once per minute in order to maintain injection from the Ring-To-Linac transport line (RTL) into the linac and from the linac into the ARC system. Both of these controls rely on information from local beam position monitors with resolutions of order 50  $\mu\text{m}$  and ignore current-dependent phenomena.

At high beam intensities transverse wakefields make the beams very sensitive to small changes in launching position and angle. As a result, beam positions must be controlled to a few microns<sup>4</sup> which is beyond the sensitivities of the local beam monitors. Furthermore, the parameters are expected to change sufficiently rapidly that the VAX control system cannot simultaneously handle the feedback load above all the other necessary control functions. Thus, a stand-alone micro-computer is needed as well as an independent feedback process.

The fast transverse feedback system has sensors at the end of the linac where the transverse beam distortions are most pronounced. The control elements are located in the  $e^+$  and  $e^-$  RTL's because the beams are most sensitive to errors (and to corrections) in the early part of the linac. As an illustration, in the absence of transverse wake fields a beam with a bunch length of 1 mm and  $5 \times 10^{10}$  particles which is injected into the linac off axis by 10  $\mu\text{m}$  at  $\beta = 10$  m will oscillate with an amplitude that damps via acceleration to about 2  $\mu\text{m}$  at 50 GeV. However, with transverse wakefields a particle behind the bunch center by  $\sigma_x/2$  will be driven to an amplitude of about 120  $\mu\text{m}$  by the end of the linac. A particle  $2\sigma_x$  behind the bunch center will have an amplitude over 1 mm. Integrating over the bunch, a 10  $\mu\text{m}$  injection error will be manifested as a 100  $\mu\text{m}$  centroid shift at the end of the linac plus tails which extend to 1 mm. The

injection conditions have been observed to vary at this level on a time scale short compared to a minute.

## Feedback Hardware

A schematic view of the fast feedback system is shown in Fig. 1. Sensors located in the last 100 m of the linac measure the beam parameters. An Intel micro-processor computes the required dipole strength changes, transmits the information through a dedicated SLCNET link, and varies eight RTL magnets. The measurements and changes can be made at 120 Hz. The details of the feedback system are shown in Fig. 2. The beam signals are obtained from either (1) four beam position monitors using eight electronics modules ( $x, x', y, y'$  for  $e^+$  and  $e^-$ ) to measure centroid shifts or (2) eight off-axis profile monitors onto which the  $e^+$  and  $e^-$  beams are diverted by pulsed magnets at approximately 1 Hz to measure shape changes. Each profile monitor was built so that the camera is always focussed on the screen, and the camera-screen combination can be moved incrementally in both directions to view a straight-ahead or a deflected beam. The resolution is about 40  $\mu\text{m}$  for both the profile monitors and the beam position monitors. Four bipolar air core dipoles of maximum strength 2.2 Gm are located in the south RTL to control positrons and four in the north for electrons. Each dipole controls one of the launch variables,  $x, x', y, y'$ . Because of space restrictions, the dipoles in a given plane partially mix position and angular variables.

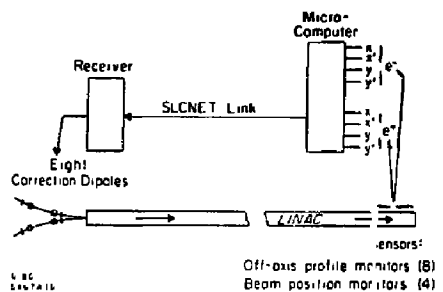


Fig. 1. Transverse feedback system for the linac.

One concern for the feedback control is whether the betatron oscillations of the beam remain coherent over the length of the linac. The coherence of the motion of all the particles is needed to make the control and sensing work over long distances. In Fig. 3 is shown a horizontal betatron oscillation induced by a dipole immediately downstream of the RTL as viewed by the position monitors along the linac. The betatron motion does remain coherent as needed by the feedback system. As can be seen, the betatron wavelength increases along the linac. It increases for two reasons: the cell length changes twice<sup>2</sup> in the first 300 m, and the quadrupole strengths saturate after 1500 m. The phase shift from the beginning to end of the linac is about 30 betatron wavelengths.

\* Work supported in part by the Department of Energy, contracts DE-AC03-76SF00515, DE-AC03-76SF00098, DE-AA03-76SF00010, and DE-AC03-81ER40050.

WASHLEK

207

60

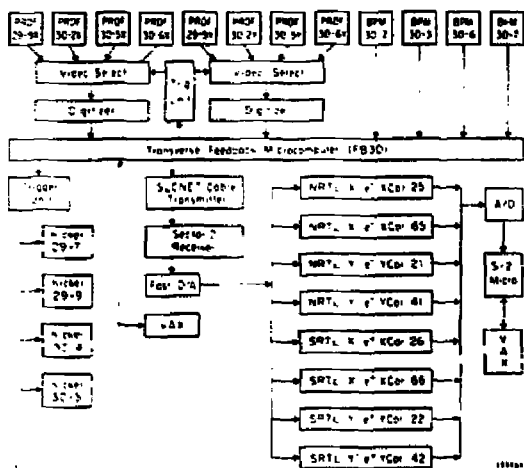


Fig. 2. Detailed components of the transverse feedback system.

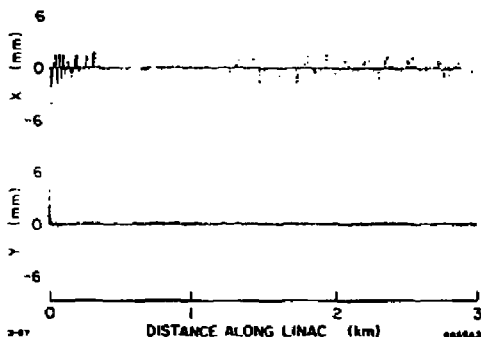


Fig. 3. Measured horizontal betatron oscillation in the linac induced by a dipole magnet early in the linac. Note that the oscillations remain coherent and that there is very little coupling, if any, to the vertical trajectory ( $6 \times 10^9 e^-$  at 42 GeV).

### Control Process

Changes in the two dipole magnets in a given beam plane in an RTL produce deflections  $\theta_a$  and  $\theta_b$  which result in beam offsets  $x_1$  and  $x_2$  at the beginning of the linac ninety degrees apart in betatron phase. These two offsets are considered the equivalent of the launch angle and position controls.

$$x_1 = \beta_a(\theta_a \beta_1)^{1/2} \sin(\phi_{1a}) + \theta_b(\beta_b \beta_1)^{1/2} \sin(\phi_{1b})$$

$$x_2 = \beta_a(\theta_a \beta_2)^{1/2} \sin(\phi_{2a}) + \theta_b(\beta_b \beta_2)^{1/2} \sin(\phi_{2b})$$

$\beta_1$  and  $\beta_2$  are the linac betatron functions at the two offset positions, and  $\beta_a$  and  $\beta_b$  are those at the dipole magnets. All  $\beta_i \approx 10\text{-}20\text{ m}$ .  $\phi$  represents the betatron phase advance from the magnet *a* or *b* to offset position 1 or 2. The magnets are located such that  $\phi_{1a} \approx \pi/2$ ,  $\phi_{1b} \approx \phi_{2b} \approx \pi$  and  $\phi_{2a} \approx 3\pi/2$ . The two offsets cause the beam to execute a betatron oscillation in the linac, produce wakefield tails, and generate signals  $S_1$  and  $S_2$  in the detectors near the end of the linac.

$$S_1 = A \left[ x_1 \cos(\phi_{f1}) + x_2 \cos\left(\phi_{f1} - \frac{\pi}{2}\right) \right]$$

$$S_2 = A \left[ x_1 \cos(\phi_{f2}) + x_2 \cos\left(\phi_{f2} - \frac{\pi}{2}\right) \right]$$

$A$  is the wakefield magnification of the injection offset.  $\phi_{f1}$  is the betatron phase advance from the injection offset ( $x_1$ ) position to the first beam sensor including the phase shift produced by the transverse wakefield.  $\phi_{f2}$  is the same phase shift but from  $x_1$  to the second sensor. The hardware was built such that under nominal lattice conditions  $\phi_{f2} \approx \phi_{f1} - \frac{\pi}{2}$ . For an SLC beam of  $5 \times 10^{11}$  particles,  $\sigma_x = 1\text{ mm}$  and 50 GeV,  $\phi_{f1} \approx 60\pi$  and  $A \approx 10$  for the BPM measurements. For the profile monitor readout, the  $A$  factor will depend upon the method used to extract the skewness of the particle distribution.

The above equations can be inverted to give a direct feedback equation

$$\begin{pmatrix} \Delta\theta_1 \\ \Delta\theta_2 \end{pmatrix} = \begin{pmatrix} a_{11} & a_{12} \\ a_{21} & a_{22} \end{pmatrix} \begin{pmatrix} \Delta S_1 \\ \Delta S_2 \end{pmatrix}$$

As was mentioned before, there are four of these feedback loops. Even though the elements  $a_{ij}$  are calculable, uncertainties in the actual beam conditions may make the wakefield calculations incorrect. Therefore, empirical measurements will most likely be needed. Changes in the beam intensity, bunchlength, energy "profile" changes along the linac from klystron changes, and RF phase changes from the energy spectrum feedback<sup>4</sup> will dynamically change the elements  $a_{ij}$  through the variables  $A$  and  $\phi_{f1}$ . Here are two examples. If the beam intensity is reduced from  $5 \times 10^{11}$  to  $4 \times 10^{11}$  for a bunch with  $\sigma_x = 1\text{ mm}$ ,  $\phi_{f1}$  shifts by 120 degrees, and  $A$  is reduced by 20%. If the linac RF phase is changed by 4 degrees with  $5 \times 10^{10}$  particles, and  $\sigma_x = 1\text{ mm}$ , then  $\phi_{f1}$  changes by 120 degrees, but  $A$  remains constant. With these likely variations, self-adaptive feedback algorithms will be needed.

### Beam Position Jitter

The feedback microcomputer has been configured to record beam positions as a function of time. Plots of  $x$  and  $y$  position jitter at the end of the linac are shown in Fig. 4. The horizontal position changes in Fig. 4(a) were associated with an energy shift caused by an intermittent klystron. Klystron cycling can produce position shifts via chromatic-dispersive effects and by RF deflections. If the motion in Fig. 4(a) is attributed to energy changes only, then  $\eta \approx 100\text{ }\mu\text{m}/0.5\% = 20\text{ mm}$ . The large position shift in Fig. 4(b) for eight pulses is due to a shift of the beam entering from the RTL, most likely an error in the timing of extraction kicker. The vertical jitter data [Fig. 4(c)] are well within specifications and has an rms value of 30  $\mu\text{m}$  which is much less than the beam height (120  $\mu\text{m}$ ). The horizontal data [Fig. 4(b)] have an rms jitter comparable to the beam width and would reduce the average luminosity by about a factor of 2. Work to reduce the transverse jitter is in progress. Data taken so far suggest that an exponentially weighted feedback would control all observed coherent position errors.<sup>5</sup>

### Transverse Shape Changes

Beam profiles at the end of the linac have been studied for wakefield and dispersive effects. The two photographs in Fig. 5 are typical beam shapes after the trajectory has been corrected to 200  $\mu\text{m}$  and the linac RF phase adjusted to make a narrow energy spectrum. The small horizontal and vertical tails can be reduced by small dipole changes in the early linac. The resulting trajectory differences are small and are not always resolvable in the BPM readings. Using this procedure, it is readily apparent that certain dipoles do not make visible wakefield tails on a particular screen, but other dipoles separated from these by about 90° in betatron phase will produce large effects. This result verifies the orthogonality of the launch controls. The entire tail cannot be removed in practice by trajectory adjustment. This is most likely due to a small remnant transverse tail on the beam entering from the RTL.

## DISCLAIMER

This report was prepared as an account of work sponsored by an agency of the United States Government. Neither the United States Government nor any agency thereof, nor any of their employees, makes any warranty, express or implied, or assumes any legal liability or responsibility for the accuracy, completeness, or usefulness of any information, apparatus, product, or process disclosed, or represents that its use would not infringe privately owned rights. Reference herein to any specific commercial product, process, or service by trade name, trademark, manufacturer, or otherwise does not necessarily constitute or imply its endorsement, recommendation, or favoring by the United States Government or any agency thereof. The views and opinions of authors expressed herein do not necessarily state or reflect those of the United States Government or any agency thereof.

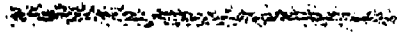
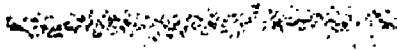
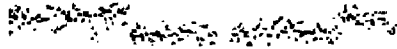


Fig. 4. Measured position jitter at the end of the linac at  $8 \times 10^9 e^-$ , 47 GeV, and 5 pps: (a) shows a horizontal position shift correctable by feedback, (b) and (c) show more typical open loop horizontal and vertical jitter plots. The horizontal jitter is  $120 \mu\text{m}$  rms and the vertical  $30 \mu\text{m}$ .

The beam image on a profile monitor can be digitized. Several contour plots are shown in Fig. 6. Figure 6(c) shows a tuned beam with a small intense core of about  $200 \mu\text{m} \times 100 \mu\text{m}$ . Figures 6(a) and 6(b) show increases in the spot dimensions due to large vertical and horizontal betatron oscillations and wakefields. The Damping Ring-RTL-Linac system is sufficiently stable so that these shapes remain the same for several minutes at a time. The time over which the beam is stable decreases with increasing current, which is consistent with the expected tighter injection tolerances. The beam profiles in Fig. 6(b) and d are due to small induced betatron oscillations and RF phase changes of a few degrees. They reveal chromatic-dispersive effects from remnant RTL dispersion, trajectory errors, and RF deflections. An RF phase change shifts the energies of the particles in different parts of the bunch, changing the energy-position correlations downstream. A small energy change can shift the

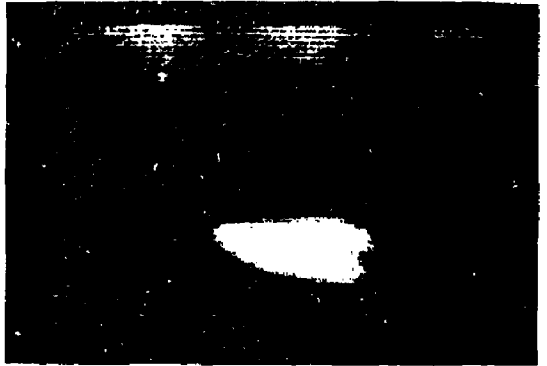
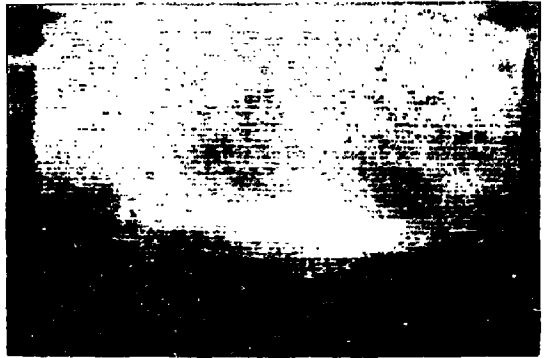


Fig. 5. Photographs of beam spots at  $1.8 \times 10^{10} e^-$  at 43 GeV. The upper photograph shows a horizontal tail on the beam core, and the lower photograph shows a vertical tail, both induced by wakefields and chromatic-dispersive effects. The fiducial holes have separations of 3 mm (h) by 1 mm (v).

place in the linac where the "dispersion" function passes through zero. Thus, beam widths on profile monitors can be narrowed using the RF phase.

In another experiment, the vertical size of the beam at the end of the linac was measured as a function of the amplitude of a betatron oscillation started early in the linac. The beam intensity was intentionally made low so that no transverse wakefields were present. The data are shown in Fig. 7. The beam size grows with increasing betatron amplitude. An estimate of the effective dispersion  $\eta$  can be made from the data via the usual equation  $\sigma_y^2 = \epsilon\beta - \eta^2\delta^2$ . The energy spread  $\delta$  was measured to be 0.5%. Therefore, the generated dispersion was 6 mm per 1 mm betatron oscillation. This result agrees with simulation results. Furthermore, measurements in the linac as the RF phase is changed show millimeter trajectory changes. As a result trajectory control will be needed in conjunction with the phase changes required by the energy spectrum feedback control.<sup>4</sup> A procedure for this correction is being studied.

#### Acknowledgments

Thanks are extended to the many people at SLAC who helped with SLAC Commissioning. Special thanks are due the Operations Group, Mechanical Engineering, and Instrumentation and Control. M.L. Arnold and Technical Illustrations kindly helped prepare this document.

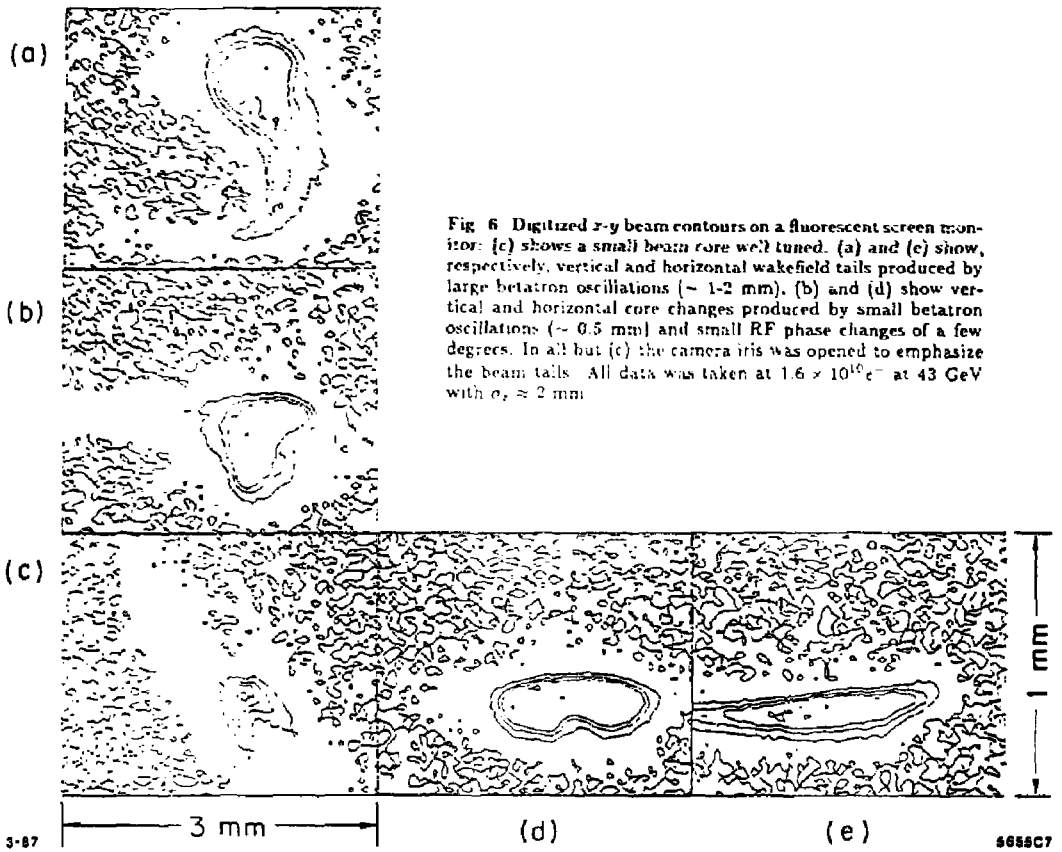


Fig 6 Digitized x-y beam contours on a fluorescent screen monitor: (c) shows a small beam core well tuned. (a) and (c) show, respectively, vertical and horizontal wakefield tails produced by large betatron oscillations ( $\sim 1-2$  mm). (b) and (d) show vertical and horizontal core changes produced by small betatron oscillations ( $\sim 0.5$  mm) and small RF phase changes of a few degrees. In all but (c) the camera iris was opened to emphasize the beam tails. All data was taken at  $1.6 \times 10^{10} e^-$  at 43 GeV with  $\sigma_y \approx 2$  mm.

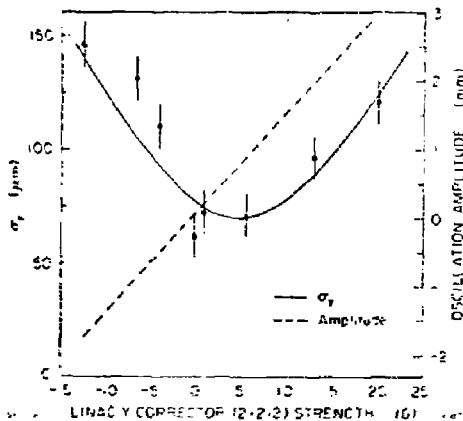


Fig. 7. Measured vertical beam size at 47 GeV as a function of the amplitude of a betatron oscillation induced by a dipole corrector early in the linac.

## References

1. J. Seeman and J. Sheppard, "Special SLC Linac Developments," 1986 Linear Accelerator Conference, SLAC, p. 214; also SLAC-PUB-3944.
2. J. Seeman *et al.*, "Experimental Beam Dynamics in the SLC Linac," 1987 Particle Accelerator Conference, Washington, D.C.; also SLAC-PUB-4181.
3. I. Almog *et al.*, "Model-Based Trajectory Optimization for the SLC," 1987 Particle Accelerator Conference, Washington, D.C.
4. G. Abrams *et al.*, "Fast Energy and Energy Spectrum Feedback in the SLC Linac," 1987 Particle Accelerator Conference, Washington, D.C.; also SLAC-PUB-4183.
5. A. Hutton suggested this efficient algorithm. An appropriate choice for this data is  $C_i = 0.2Y_i + 0.8C_{i-1}$ , where for pulse  $i$ ,  $Y_i$  is the measurement and  $C_i$  is the control. Values of  $Y_i$  more than ten sigma from the mean are rejected.